Molecular Pharmacology Fast Forward. Published on February 12, 2016 as DOI: 10.1124/mol.115.102657
This article has not been copyedited and formatted. The final version may differ from this version.

Molecular basis of ligand dissociation from the adenosine A_{2A} receptor*

Dong Guo, Albert C. Pan, Ron O. Dror, Tamara Mocking, Rongfang Liu, Laura H. Heitman, David E. Shaw, Adriaan P. IJzerman

Affiliations:

Division of Medicinal Chemistry, Leiden Academic Centre for Drug Research (LACDR), Leiden University, P.O. Box 9502, 2300 RA Leiden, the Netherlands: DG, TM, RL, LHH, APIJ.

D. E. Shaw Research, New York, NY 10036, USA: ACP, ROD, DES.

Department of Biochemistry and Molecular Biophysics, Columbia University, New York, NY 10032, USA: DES

Molecular Pharmacology Fast Forward. Published on February 12, 2016 as DOI: 10.1124/mol.115.102657
This article has not been copyedited and formatted. The final version may differ from this version.

Running title: ligand unbinding from G protein-coupled receptor

Corresponding author:

Adriaan P. IJzerman

Gorlaeus Lab/LACDR, Leiden University, Dept. Medicinal Chemistry, Room L072, Einsteinweg 55, 2333 CC Leiden, The Netherlands.

Phone: +31(0)71 527 4651

Fax: +31 (0) 71 527 4277

E-mail: ijzerman@lacdr.leidenuniv.nl

Number of text pages: **29**

Number of tables: **2**

Number of figures: **3**

Number of references: **28**

Number of words in the Abstract: **115**

Number of words in the introduction: **270**

Number of words in the discussion: **1155**

Molecular Pharmacology Fast Forward. Published on February 12, 2016 as DOI: 10.1124/mol.115.102657
This article has not been copyedited and formatted. The final version may differ from this version.

List of nonstandard abbreviations

$A_{2A}R$, adenosine A_{2A} receptor; ADA, adenosine deaminase; BCA, bicinchoninic acid; DMEM, Dulbecco's modified Eagle's medium; GPCR, G protein-coupled receptors; MD, molecular dynamics; TAMD, temperature accelerated molecular dynamics; RT, residence time; TIP3P, three-point water model; TMB, 3, 3', 5, 5'-tetramethyl-benzidine; ZM241385, 4-(2-[7-Amino-2-(2-furyl)[1,2,4]triazolo[2,3-*a*][1,3,5]triazin-5-ylamino]ethyl)phenol.

Molecular Pharmacology Fast Forward. Published on February 12, 2016 as DOI: 10.1124/mol.115.102657
This article has not been copyedited and formatted. The final version may differ from this version.

Abstract

How drugs dissociate from their targets is largely unknown. We investigated the molecular basis of this process in the adenosine A_{2A} receptor ($A_{2A}R$), a prototypical G protein-coupled receptor. Through kinetic radioligand binding experiments, we characterized mutant receptors selected based on molecular dynamics simulations of the antagonist ZM241385 dissociating from the $A_{2A}R$. We discovered mutations that dramatically altered the ligand's dissociation rate despite only marginally influencing its binding affinity, demonstrating that even receptor features with little contribution to affinity may prove critical to the dissociation process. Our results also suggest that ZM241385 follows a multi-step dissociation pathway, consecutively interacting with distinct receptor regions, a mechanism that may also be common to many other G protein-coupled receptors.

Molecular Pharmacology Fast Forward. Published on February 12, 2016 as DOI: 10.1124/mol.115.102657
This article has not been copyedited and formatted. The final version may differ from this version.

Introduction

G protein-coupled receptors (GPCRs) represent the largest class of drug targets; they are home for one-third of all marketed drugs (Overington et al., 2006). Recent developments in this field have yielded several crystal structures that provide an atomic view on the ligand-receptor interaction (Katritch et al., 2013). This is vital information for molecular understanding of the ligand-receptor interaction. However, the knowledge gained is largely 'frozen' in nature and only reflects the final interaction at the ligand-binding site. How a ligand dissociates from its binding pocket and which residues are involved in this dynamic process are still largely unknown. Here, we chose the human adenosine A_{2A} receptor ($A_{2A}R$), a prototypical GPCR, for such a mechanistic exploration. We applied molecular dynamics (MD) simulations to the crystal structure of the $A_{2A}R$ (PDB ID: 4EIY) (Liu et al., 2012) to help in the selection of amino acid residues that have potential interactions with the crystallographic ligand, ZM241385, along its dissociation pathway from the receptor. The identified residues, many of which were not in contact with the ligand in the crystal structure, were subsequently mutated and the resulting mutant receptors were then subjected to experimental determination of the ligand's affinity and dissociation kinetics. We observed that the $E169^{ECL2}Q$, $H264^{7.29}A$ and $T256^{6.58}A$ mutants accelerated ZM241385's dissociation from the receptors and the $I66^{2.63}A$, $S67^{2.64}A$, $K153^{ECL2}A$ and $L267^{7.32}A$ mutants slowed down the process. Interestingly, these mutations only minimally influenced ZM241385's binding affinity. Our results also suggest that ZM241385 follows a multi-step dissociation pathway, consecutively interacting with topographically distinct regions of the receptor. We speculate that such a multi-step dissociation process may be common to other GPCRs as well.

Molecular Pharmacology Fast Forward. Published on February 12, 2016 as DOI: 10.1124/mol.115.102657
This article has not been copyedited and formatted. The final version may differ from this version.

Materials and Methods

Chemicals and reagents

[^{3}H]-ZM241385 (specific activity 47.7 Ci · mmol^{-1}) was purchased from ARC Inc. (St. Louis, MO, USA). ZM241385 was a gift from Dr. S. M. Poucher (Astra Zeneca, Macclesfield, UK). Adenosine deaminase (ADA) was purchased from Boehringer Mannheim (Manheim, Germany). Bicinchoninic acid (BCA) and BCA protein assay reagent were obtained from Pierce Chemical Company (Rockford, IL, USA). All other chemicals were of analytical grade and obtained from standard commercial sources.

Molecular dynamics

MD simulations of the ZM241385-A_{2A}R complex were performed on a special-purpose machine, Anton (Shaw et al., 2009). The simulation system was prepared and equilibrated following the protocols detailed in (Kruse et al., 2012). Briefly, the system was prepared using the crystallized complex of Protein Data Bank (PDB) ID 4EIY solvated in approximately 14,000 TIP3P (three-point water model) water molecules (MacKerell et al., 1998), 28 sodium ions, 38 chloride ions, and 134 DPPC lipids in a 72-Å^3 box consisting of approximately 65,000 atoms. The prepared system was minimized and equilibrated as previously described (Kruse et al., 2012).

We then ran 10 temperature accelerated molecular dynamics (TAMD) simulations (Maragliano and Vanden-Eijnden, 2006) of the ZM241385 ligand dissociating from the A_{2A} receptor, starting from the equilibrated snapshot of the ligand-receptor complex with different random initial velocities. Trajectories ended with the ligand completely dissociated from the receptor. TAMD is a method for enhancing sampling along a chosen set of collective variables (CVs; e.g., the center-of-mass of a group of atoms). The acceleration is achieved by harmonically tethering a CV to a fictitious particle undergoing Brownian motion at a higher temperature. With a proper choice of

Molecular Pharmacology Fast Forward. Published on February 12, 2016 as DOI: 10.1124/mol.115.102657
This article has not been copyedited and formatted. The final version may differ from this version.

parameters, the sampling of the chosen CV is accelerated such that the fictitious particles still obey Boltzmann statistics at the higher, fictitious temperature, $\bar{T}$, while the non-accelerated orthogonal degrees of freedom of the real system remain properly distributed at the real temperature. In the TAMD simulations, the center-of-mass of the heavy atoms of the ZM241385 ligand was accelerated to encourage ligand dissociation. The spring constant tethering the center-of-mass CV to the fictitious particle was 100 kcal·mol^{-1}·Å^{-2}. The friction coefficient for the fictitious particle was 100 ps kcal mol^{-1} Å^{-2}, and the fictitious temperature, $k_B\bar{T}$, was 2.4 kcal·mol^{-1}. To fix the position and orientation of $A_{2A}R$, the receptor was weakly restrained with harmonic restraints on the x-,y-,z-positions of Cα atoms in the intracellular region (residues 22 to 29, 43 to 48, 122 to 128, 97 to 102, 193 to 200, 233 to 238, and 284 to 290) with a force constant of 0.5 kcal·mol^{-1}·Å^{-2}. These simulations were run in the NPT ensemble at 310 K (37 ^{o}C) and 1 bar. A flat-bottom harmonic distance restraint between the center-of-mass of the ligand and the initial position of the ligand in the binding pocket was maintained throughout the simulations with the harmonic region beginning 30 Å away from the binding pocket with a force constant of 100 kcal·mol^{-1}·Å^{-2}.

Site directed mutagenesis

Site-directed mutants were constructed by PCR mutagenesis using pcDNA3.1-hA_{2A}R with N-terminal HA and FLAG tags and C-terminal His tag as a template. The mutants E169A and E169Q were generated by Baseclear (Leiden, The Netherlands) and the other mutants were created in house as follows. Mutant primers for directional PCR product cloning were designed using the online Quickchange® primer design program (Agilent Technologies) and primers were

Molecular Pharmacology Fast Forward. Published on February 12, 2016 as DOI: 10.1124/mol.115.102657
This article has not been copyedited and formatted. The final version may differ from this version.

obtained from Eurogentec® (Maastricht, The Netherland). All DNA sequences were verified by Sanger sequencing at LGTC (Leiden, the Netherlands).

Cell culture, transfection and enzyme-linked immunosorbent assay (ELISA)

We followed procedures as described previously (Lane et al., 2012). Briefly, human embryonic kidney (HEK) 293 cells were grown as monolayers in Dulbecco's modified Eagle's medium (DMEM) supplemented with stable glutamine, 10% newborn calf serum, streptomycin, and penicillin at 37 °C in a moist, 7% CO_2 atmosphere. The cells were transfected with plasmid DNA using a calcium phosphate method followed by 48 h incubation before membrane preparation. For ELISA assay, 24 h after transfection, cells were split into 96-well poly-D-lysine-coated plates at a density of 1×10^6 cells per well. After an additional 24 h, the cells were fixed with 4% formaldehyde and then washed with PBS before adding the primary antibody, monoclonal M2-anti-FLAG antibody (1:1000) and incubating for 30 min at 37 °C. Next, the antibody was removed and the cells were washed with DMEM/25 mM HEPES before adding the second antibody, monoclonal anti-Mouse-HRP 1:5000 and incubating for 30 min at 37 °C. After removing the second antibody and washed the cells with warm PBS, 3, 3', 5, 5'-tetramethyl-benzidine (TMB) was added and incubated for 5 min in the dark. The reaction was stopped with 1 M H_3PO_4 and absorbance was read at 450 nm using a Victor^2 plate reader (PerkinElmer Life and Analytical Sciences).

Membrane preparation

Cells were detached from the plates by scraping into PBS. Cells were collected and centrifuged at 700×g (3000 r.p.m.) for 5 min. Pellets from 10 plates (10 cm ø) were pooled and resuspended in 8 mL ice cold buffer containing 50 mM Tris-HCl, pH 7.4. Cell suspension was homogenized

Molecular Pharmacology Fast Forward. Published on February 12, 2016 as DOI: 10.1124/mol.115.102657
This article has not been copyedited and formatted. The final version may differ from this version.

with an UltraThurrax homogenizer (Heidolph Instruments, Schwabach, Germany). Cell suspension was centrifuged at 100,000×g (31000 r.p.m.) in a Beckman Optima LE-80K ultracentrifuge at 4 °C for 20 min. The pellet was resuspended in 4 mL of Tris buffer and the homogenization and centrifugation step was repeated. After this, Tris buffer (2 mL) was used to resuspend the pellet and ADA was added (0.8 IU/mL) to break down endogenous adenosine. Membranes were stored in 200 µL aliquots at -80 ˚C. Membrane protein concentrations were measured using the BCA (bicinchoninic acid) method(Smith et al., 1985).

Radioligand homologous displacement assay

Radioligand displacement experiments were performed with membranes of HEK293 cells expressing the wild-type or mutant human adenosine A_{2A} receptor using eleven concentrations of unlabeled ZM241385 (from 10^{-12} M to 10^{-6} M) in the presence of 2.8 nM [^{3}H]-ZM241385 at 4 ˚C (Guo et al., 2014). Membrane aliquots containing 2.5-5.0 µg of protein were incubated in a total volume of 100 µl of assay buffer (50 mM Tris-HCl, pH 7.4, supplemented with 5 mM $MgCl_2$) to adjust the assay window to approximately 3000 DPM. Nonspecific binding was determined in the presence of 10 µM ZM241385 and represented less than 10% of the total binding. [^{3}H]-ZM241385 did not bind specifically to membranes prepared from parental HEK293 cells. Incubations were terminated by rapid vacuum filtration to separate the bound and free radioligand through 96-well GF/B filter plates using a Perkin Elmer Filtermate-harvester (Perkin Elmer, Groningen, Netherlands) after 2 h incubation to ensure the equilibrium was reached at all concentrations of radioligand. Filters were subsequently washed three times with 2 ml of ice-cold buffer. The filter-bound radioactivity was determined by scintillation spectrometry using a P-E 1450 Microbeta Wallac Trilux scintillation counter (Perkin Elmer, Groningen, Netherlands).

Molecular Pharmacology Fast Forward. Published on February 12, 2016 as DOI: 10.1124/mol.115.102657
This article has not been copyedited and formatted. The final version may differ from this version.

Radioligand dissociation assays

Dissociation experiments of [^{3}H]-ZM241385 on the wild-type or mutant adenosine A_{2A} receptors were performed by pre-incubating membrane suspension with [^{3}H]-ZM241385 in 100 µl of assay buffer at 4 °C for 2 h (Guo et al., 2012). After the pre-incubation, the dissociation was initiated by addition of 1 µM of unlabeled ZM241385 in 5 µL. The amount of radioligand still bound to the receptor was measured at various time intervals for a total duration of 2 h to 4 h at 4 ˚C to ensure that [^{3}H]-ZM241385 was fully dissociated from the wild-type or mutant adenosine A_{2A} receptors. Incubations were terminated and samples were obtained as described under *Radioligand homologous displacement assays*.

Data analysis

Residue superscripts refer to the Ballesteros-Weinstein numbering (Ballesteros and Weinstein, 1995) in which a single most conserved residue among the class A GPCRs is designated x.50, where x is the transmembrane helix number. All other residues on that helix are numbered relative to this conserved position. All experimental data was analyzed by using GraphPad Prism 5.0 (GraphPad Software Inc., San Diego, CA). Values obtained are mean ± s.e.m of at least three independent experiments performed in duplicate for (kinetic) radioligand binding assays and of at least three independent experiments performed in quadruplicate for an ELISA assay. IC_{50} values were obtained from radioligand homologous displacement assays, and pK_i values were calculated using a *one site–homologous* model. Dissociation data were fitted using a model of *one-phase exponential decay* to obtain k_{off}. The residence time (RT) was calculated using RT = 1 / k_{off} (Copeland, 2005). Statistical analysis was performed using one-way ANOVA with Dunnett's test (*$P < 0.05$, **$P < 0.01$, ***$P < 0.001$, **** $P < 0.0001$).

Molecular Pharmacology Fast Forward. Published on February 12, 2016 as DOI: 10.1124/mol.115.102657
This article has not been copyedited and formatted. The final version may differ from this version.

Results

Molecular dynamics

We performed ten simulations of the dissociation of ZM241385 from $A_{2A}R$ using temperature accelerated molecular dynamics (TAMD), a method for enhanced sampling along a chosen set of collective variables (Maragliano and Vanden-Eijnden, 2006). Here, TAMD was used to accelerate the center-of-mass of the ligand by tethering it to a fictitious particle at a higher temperature (see Methods). This tethering increases the energy available to the ligand, allowing it to surmount barriers along the dissociation pathway more quickly. Because we are only accelerating the ligand, the rest of the system should be minimally affected and we expect that the observed dissociation pathways should be qualitatively similar—though not necessarily identical—to unbiased dissociation pathways. In particular, protein motions are not enhanced, so we do not expect the conformation of the receptor to be substantially affected. The kinetics of the dissociation process, however, are dramatically accelerated, allowing us to simulate ligand dissociation on computationally tractable timescales.

Each TAMD trajectory began with an equilibrated 'snapshot' of the ligand-receptor complex based on the 1.8 Å crystal structure (PDB ID: 4EIY) with different random initial velocities and ended with the ligand completely dissociated from the receptor. Dissociation of ZM241385 from the receptor began between 20 and 300 ns into the TAMD trajectories and typically took 20 ns to complete.

To identify residues that may influence the binding kinetics, we searched for contacts between ZM241385 (Fig. 1 inset) and the protein during ligand dissociation. A contact was identified when either the oxygen atom in ZM241385's furan ring or the nitrogen atom in ZM241385's exocyclic primary amine group was within 4 Å of the backbone nitrogen or carbonyl oxygen of a receptor residue. In total, 16 residues were identified (Table 1). They are located in the upper part

Molecular Pharmacology Fast Forward. Published on February 12, 2016 as DOI: 10.1124/mol.115.102657
This article has not been copyedited and formatted. The final version may differ from this version.

of the receptor, in either the transmembrane helices or the extracellular loops. Many of the identified contacts involved ligand-receptor interactions that were not seen in the crystal structure. We note that we would not necessarily expect all of these residues to influence the ligand's off-rate; that rate will depend primarily on the free energy difference between the bound state and the highest-energy state along the dissociation pathway (the transition state), and we would not expect that every residue that interacts with the ligand during the dissociation process will influence the energies of these two states. These residues do, however, represent a useful starting point for further experimental investigation.

We also observed that ZM241385 adopted several metastable poses in the dissociation simulations before completely unbinding (Fig. 1). In most of the trajectories, for example, the ligand paused transiently near H2 and H7, close to I66$^{2.63}$, S67$^{2.64}$, L267$^{7.32}$ and Y271$^{7.36}$, before dissociating from the receptor.

The affinity of [^{3}H]-ZM241385 at the wild-type and mutant A_{2A}Rs

We individually mutated 12 receptor residues of interest from the 16 residues suggested by the MD simulations (Table 1), mostly to alanine, and then assessed the affinity of ZM241385 for these receptor variants (mutations to the remaining 4 residues were not considered, because these residues were either small side-chain residues [G-1$^{N\text{-term}}$, A265$^{7.30}$ and G152^{ECL2}] or proline [P266$^{7.31}$]). Prior to the binding experiments, we determined the expression level of the transiently transfected receptors at the cell surface. None of the mutant receptors (13 mutants in total) was found to express at a level significantly different from the transiently transfected wild-type (WT) receptor (i.e., $p > 0.05$ in all cases, one-way ANOVA) (Fig. 2A).

Next, radioligand homologous displacement experiments were performed to determine the affinity (pK_i) values of ZM241385 for the WT and mutant A_{2A}Rs. [^{3}H]-ZM241385 was able to

Molecular Pharmacology Fast Forward. Published on February 12, 2016 as DOI: 10.1124/mol.115.102657
This article has not been copyedited and formatted. The final version may differ from this version.

bind to 11 of the 13 mutants (Table 2) with relatively high affinity. The two exceptions were E169^{ECL2}A and Y271$^{7.36}$A, which showed negligible [^{3}H]-ZM241385 binding. ZM241385 was able to bind to the E169^{ECL2}Q mutant, but with lower affinity than the WT receptor (pK_i = 7.46 for E169^{ECL2}Q compared to pK_i = 7.83 for WT, Table 2; Fig. 2B). The ligand also bound to the T256$^{6.58}$A mutant with lower affinity (pK_i = 7.43, Table 2; Fig. 2B) and to the Q157^{ECL2}A with a slightly increased affinity (pK_i = 8.03, Table 2) relative to the WT receptor. The remaining mutants displayed affinity similar to that of the WT receptor.

The dissociation of [^{3}H]-ZM241385 from the wild-type and mutant A_{2A}R

We then performed radioligand dissociation assays and determined the dissociation rate constant (k_{off}) of ZM241385 from the wild-type and mutant adenosine A_{2A} receptors. The results are detailed in Table 2. Notably, ZM241385 displayed a dramatically decreased residence time ($1/k_{off}$) of just a few minutes at these three mutants compared to the wild-type receptor (84 min), as was evident from the significant leftward shift of the dissociation curves to shorter times (Fig. 2C). In stark contrast, on four other mutants, namely I66$^{2.63}$A, S67$^{2.64}$A, K153^{ECL2}A and L267$^{7.32}$A, significantly increased residence times of ZM241385 were observed (141 ± 2 min, 130 ± 4 min, 106 ± 3 min and 196 ± 5 min, respectively). All other mutants displayed receptor residence times and dissociation rates that were similar to those at the wild type (Table 2).

Unlike our MD simulations, which included a physiological concentration of sodium (~150 mM), the kinetic radioligand binding experiments described above did not include sodium. As a control, we also measured the dissociation rate of ZM241385 from the WT and the H264$^{7.29}$A receptors in the presence of 150 mM NaCl. Dissociation from both constructs was slowed by the presence of sodium (data not shown), but the dissociation kinetics from the H264$^{7.29}$A mutant remained much faster (i.e., 8-fold) than from the WT receptor, as was observed in the absence of sodium ions (i.e.,

Molecular Pharmacology Fast Forward. Published on February 12, 2016 as DOI: 10.1124/mol.115.102657
This article has not been copyedited and formatted. The final version may differ from this version.

19-fold). We expect that the presence or absence of sodium will not typically change the qualitative effects of the mutants relative to the WT.

Molecular Pharmacology Fast Forward. Published on February 12, 2016 as DOI: 10.1124/mol.115.102657
This article has not been copyedited and formatted. The final version may differ from this version.

Discussion

In this study we addressed the exit pathway of a drug from its target. We started from a crystal structure of a GPCR, being the most prevalent drug targets (Overington et al., 2006), with its co-crystallized ligand. At the time we conducted our study, one crystal structure stood out due to its high resolution (1.8 Å), the $A_{2A}R$ bound to the antagonist ZM241385 (PDB ID: 4EIY).

Growing computer power, as well as improved software and computer hardware for molecular dynamics simulations (Durrant and McCammon, 2011; Shaw et al., 2009), have made such simulations increasingly useful (Dror et al., 2012). Such simulations have been used to study both association and dissociation of ligands to various proteins, including GPCRs (Dror et al., 2011; Hurst et al., 2010; Kruse et al., 2012; Wang and Duan, 2007). In this study, molecular dynamics simulations helped us identify several amino acid residues (Table 2) that upon mutation showed a minimal effect on ZM241385's equilibrium binding affinity while having a major impact on its dissociation kinetics.

Notably, most of the selected residues would have gone unnoticed in a more classical site-directed mutagenesis study with a primary emphasis on loss- or gain-of-affinity mutations. Indeed, of the 13 mutants generated, only two had been reported previously for loss of affinity. One is $E169^{ECL2}$, which was identified to interact through direct H-bonding with ZM241385 (Jaakola et al., 2008). Upon mutation of this residue to alanine (A) ZM241385 displayed no binding at the receptor, as shown previously (Kim et al., 1996). However, when changing it to glutamine (Q) the binding of ZM241385 was restored, most likely due to preserved hydrogen bonding to the ligand. Likewise, $Y271^{7.36}A$ disrupted ZM241385 binding, probably due to the loss of its π-π stacking interaction with the antagonist's phenol group. The importance of $Y271^{7.36}A$ had also been reported for the binding of the $A_{2A}R$ agonist CGS21680 and the

Molecular Pharmacology Fast Forward. Published on February 12, 2016 as DOI: 10.1124/mol.115.102657
This article has not been copyedited and formatted. The final version may differ from this version.

antagonist XAC (Kim et al., 1995). Other than at these two mutants, ZM241384 displayed very similar binding affinities for the remaining ten mutant receptors (Table 2). Again, such 'similar-function' mutants might be overlooked for further mechanistic investigations if affinity alone were taken into account.

Kinetic rather than equilibrium radioligand binding studies revealed that several residues are of great importance in determining ZM241385's dissociation characteristics, particularly three residues (E169^{ECL2}, T256$^{6.58}$ and H264$^{7.29}$) located at the intersection of the binding cavity and the extracellular loops. We observed that ZM241385 dissociated from these mutated receptors much faster than from the wild-type $A_{2A}R$ (less than 5 min vs. 84 min, Table 2). Four other mutants, namely I66$^{2.63}$A, S67$^{2.64}$A, K153^{ECL2}A and L267$^{7.32}$A, significantly decreased the dissociation rate of ZM241385. None of these residues, except for E169^{ECL2}, is located in the binding pocket of ZM241385, which is formed by residues in the upper part of transmembrane helices 5, 6 and 7 (Jaakola and IJzerman, 2010; Liu et al., 2012). These residues may form transient interactions with ZM241385 that contribute to the energetic barriers on the dissociation pathway, although we cannot exclude the possibility that the mutations act instead by influencing the global conformation of the receptor. Interestingly, the mutants that accelerated or slowed down ligand dissociation are located in two topographically different clusters in the $A_{2A}R$ crystal structure, one formed by E169^{ECL2}, T256$^{6.58}$ and H264$^{7.29}$, the other by I66$^{2.63}$, S67$^{2.64}$, and L267$^{7.32}$ (Fig. 3A). The dissociation of ZM241385 from the $A_{2A}R$ may thus follow a multi-step dissociation pathway, with the ligand consecutively moving from one cluster to another.

The molecular dynamics simulations of ZM241385's egress from the $A_{2A}R$ further support the experimental observations and our speculation that the unbinding process of the ligand is multi-step. In the 4EIY crystal structure from which our simulations were initiated, the residues whose mutation accelerates dissociation form a 'triad' interacting with ZM241385 through hydrogen

Molecular Pharmacology Fast Forward. Published on February 12, 2016 as DOI: 10.1124/mol.115.102657
This article has not been copyedited and formatted. The final version may differ from this version.

bonding together with a structural water molecule (W2517) (Fig. 3A). This intact triad is in agreement with ZM241385's relatively long residence time at the wild-type $A_{2A}R$ (84 min) and short residence times at the E169^{ECL2}Q, T256$^{6.58}$A and H264$^{7.29}$A mutants in which the triad is disturbed (all residence times less than 5 min). In the molecular dynamics simulations, the breaking of the interaction between H264$^{7.29}$, E169^{ECL2} and the ligand—a motion loosening the hydrogen bond network formed by the 'triad' and enlarging the opening of the binding pocket (Fig. 3B)—preceded dissociation. Mutating residues in this cluster loosens the hydrogen bond network, thus facilitating further movement of ZM241385 towards the extracellular space (Table 2, Fig. 2C). These results are consistent with a previous observation that the interaction between H264$^{7.29}$ and E169^{ECL2} leads to low mobility of the extracellular loops. These residues were suggested to act as part of a "lid" closing the binding site and stabilizing the $A_{2A}R$/ZM241385 complex (Rodríguez et al., 2011). Intriguingly, such a "lid" is reminiscent of that reported at other GPCRs, e.g., the M_3 muscarinic receptor (M_3R). In that receptor, tiotropium—the co-crystalized ligand—is buried within the binding pocket and is shielded by a cluster of tyrosine residues (Y148$^{3.33}$, Y506$^{6.51}$ and Y529$^{7.39}$) from the solvent at the extracellular side (Kruse et al., 2012). Such a lid almost completely prevents the influx of water molecules to hydrate tiotropium, an essential step for ligand dissociation (Bortolato et al., 2013; Schmidtke et al., 2011). This is in accordance with tiotropium's long residence time on the M_3R (more than 24 h) (Casarosa et al., 2009). Not surprisingly, mutation of one of the tyrosine residues significantly influenced tiotropium's dissociation half-life (reducing it to less than 10 min) (Tautermann et al., 2013). We speculate that the triad in the $A_{2A}R$ similarly retains ZM241385 in the binding pocket; a concerted movement of the triad residues into different rotamer configurations is necessary to loosen the ligand from its tightly bound state.

Molecular Pharmacology Fast Forward. Published on February 12, 2016 as DOI: 10.1124/mol.115.102657
This article has not been copyedited and formatted. The final version may differ from this version.

An alternative binding intermediate along the dissociation pathway in the MD simulations involved ZM241385 interacting with I66$^{2.63}$, S67$^{2.64}$, and L267$^{7.32}$. This forces ZM241385 to assume a pose similar to the one observed in another A_{2A}R-ZM241385 crystal structure (PDB ID: 3PWH) (Dore et al., 2011), where the antagonist's phenol group projected into the domain mentioned above (I66$^{2.63}$, S67$^{2.64}$, and L267$^{7.32}$). Mutation of these residues into much smaller alanine reduces steric hindrance and increases the ligand's freedom of rotation. As a result, ZM241385 displayed significantly increased residence times at these three mutant receptors (Fig. 2C, Table 2).

Taken together, our biochemical and computational results provide a molecular description of the dissociation of ZM241385 from the A_{2A}R. The ligand appears to follow a multi-step pathway, first breaking the hydrogen bond network formed by the triad of E169^{ECL2}, T256$^{6.58}$ and H264$^{7.29}$ and transiently contacting the quite hydrophobic pocket above Y271$^{7.36}$ consisting of I66$^{2.63}$, S67$^{2.64}$, and L267$^{7.32}$ before moving further away from the binding pocket into the extracellular domain and bulk solvent. We believe that atomic-level descriptions of the kinetic process as in this study will deepen our understanding of ligand-GPCR interactions and will lay the structural foundation for future rational design of drugs with optimized binding kinetics.

Molecular Pharmacology Fast Forward. Published on February 12, 2016 as DOI: 10.1124/mol.115.102657
This article has not been copyedited and formatted. The final version may differ from this version.

Acknowledgments

We thank Hillary Green for assistance with simulation setup. We thank Henk de Vries for assistance with the kinetic radioligand binding assay.

Molecular Pharmacology Fast Forward. Published on February 12, 2016 as DOI: 10.1124/mol.115.102657
This article has not been copyedited and formatted. The final version may differ from this version.

Authorship Contributions

Participated in research design: DG, ACP, ROD, LHH, DES, APIJ

Conducted experiments: DG, ACP, ROD, TM, RL

Performed data analysis: DG, ACP, ROD, TM

Wrote or contributed to the writing of the manuscript: DG, ACP, ROD, LHH, DES, APIJ

Molecular Pharmacology Fast Forward. Published on February 12, 2016 as DOI: 10.1124/mol.115.102657
This article has not been copyedited and formatted. The final version may differ from this version.

References

Ballesteros J and Weinstein H (1995) Integrated methods for the construction of three-dimensional models and computational probing of structure-function relations in G protein-coupled receptors, in *Methods Neurosci* pp 366-428, Elsevier.

Bortolato A, Tehan BG, Bodnarchuk MS, Essex JW and Mason JS (2013) Water network perturbation in ligand binding: adenosine A_{2A} antagonists as a case study. *J Chem Inf Model* **53**(7): 1700-1713.

Casarosa P, Bouyssou T, Germeyer S, Schnapp A, Gantner F and Pieper M (2009) Preclinical evaluation of long-acting muscarinic antagonists: comparison of tiotropium and investigational drugs. *J Pharmacol Exp Ther* **330**(2): 660-668.

Copeland RA (2005) *Evaluation of enzyme inhibitors in drug discovery: A guide for medicinal chemists and pharmacologists*. 2005/12/15 ed. Wiley, New York.

Dore AS, Robertson N, Errey JC, Ng I, Hollenstein K, Tehan B, Hurrell E, Bennett K, Congreve M, Magnani F, Tate CG, Weir M and Marshall FH (2011) Structure of the adenosine A_{2A} receptor in complex with ZM241385 and the xanthines XAC and caffeine. *Structure* **19**(9): 1283-1293.

Dror RO, Dirks RM, Grossman JP, Xu H and Shaw DE (2012) Biomolecular simulation: a computational microscope for molecular biology. *Annu Rev Biophys* **41**: 429-452.

Dror RO, Pan AC, Arlow DH, Borhani DW, Maragakis P, Shan Y, Xu H and Shaw DE (2011) Pathway and mechanism of drug binding to G-protein-coupled receptors. *Proc Natl Acad Sci U S A* **108**(32): 13118-13123.

Durrant JD and McCammon JA (2011) Molecular dynamics simulations and drug discovery. *Bmc Biol* **9**.

Molecular Pharmacology Fast Forward. Published on February 12, 2016 as DOI: 10.1124/mol.115.102657
This article has not been copyedited and formatted. The final version may differ from this version.

Guo D, Mulder-Krieger T, IJzerman AP and Heitman LH (2012) Functional efficacy of adenosine A_{2A} receptor agonists is positively correlated to their receptor residence time. *Br J Pharmacol* **166**(6): 1846-1859.

Guo D, Xia L, van Veldhoven JP, Hazeu M, Mocking T, Brussee J, Ijzerman AP and Heitman LH (2014) Binding kinetics of ZM241385 derivatives at the human adenosine A2A receptor. *ChemMedChem* **9**(4): 752-761.

Humphrey W, Dalke A and Schulten K (1996) VMD: visual molecular dynamics. *J Mol Graph* **14**(1): 33-38, 27-38.

Hurst DP, Grossfield A, Lynch DL, Feller S, Romo TD, Gawrisch K, Pitman MC and Reggio PH (2010) A Lipid Pathway for Ligand Binding Is Necessary for a Cannabinoid G Protein-coupled Receptor. *J Biol Chem* **285**(23): 17954-17964.

Jaakola VP, Griffith MT, Hanson MA, Cherezov V, Chien EY, Lane JR, IJzerman AP and Stevens RC (2008) The 2.6 angstrom crystal structure of a human A_{2A} adenosine receptor bound to an antagonist. *Science* **322**(5905): 1211-1217.

Jaakola VP and IJzerman AP (2010) The crystallographic structure of the human adenosine A(2A) receptor in a high-affinity antagonist-bound state: implications for GPCR drug screening and design. *Curr Opin Struct Biol* **20**(4): 401-414.

Katritch V, Cherezov V and Stevens RC (2013) Structure-function of the G protein-coupled receptor superfamily. *Annu Rev Pharmacol Toxicol* **53**: 531-556.

Kim J, Jiang Q, Glashofer M, Yehle S, Wess J and Jacobson KA (1996) Glutamate residues in the second extracellular loop of the human A_{2a} adenosine receptor are required for ligand recognition. *Mol Pharmacol* **49**(4): 683-691.

Molecular Pharmacology Fast Forward. Published on February 12, 2016 as DOI: 10.1124/mol.115.102657
This article has not been copyedited and formatted. The final version may differ from this version.

Kim J, Wess J, van Rhee AM, Schoneberg T and Jacobson KA (1995) Site-directed mutagenesis identifies residues involved in ligand recognition in the human A_{2a} adenosine receptor. *J Biol Chem* **270**(23): 13987-13997.

Kruse AC, Hu J, Pan AC, Arlow DH, Rosenbaum DM, Rosemond E, Green HF, Liu T, Chae PS, Dror RO, Shaw DE, Weis WI, Wess J and Kobilka BK (2012) Structure and dynamics of the M_3 muscarinic acetylcholine receptor. *Nature* **482**(7386): 552-556.

Lane JR, Klein Herenbrink C, van Westen GJ, Spoorendonk JA, Hoffmann C and IJzerman AP (2012) A novel nonribose agonist, LUF5834, engages residues that are distinct from those of adenosine-like ligands to activate the adenosine A_{2a} receptor. *Mol Pharmacol* **81**(3): 475-487.

Liu W, Chun E, Thompson AA, Chubukov P, Xu F, Katritch V, Han GW, Roth CB, Heitman LH, IJzerman AP, Cherezov V and Stevens RC (2012) Structural basis for allosteric regulation of GPCRs by sodium ions. *Science* **337**(6091): 232-236.

MacKerell AD, Bashford D, Bellott M, Dunbrack RL, Evanseck JD, Field MJ, Fischer S, Gao J, Guo H, Ha S, Joseph-McCarthy D, Kuchnir L, Kuczera K, Lau FT, Mattos C, Michnick S, Ngo T, Nguyen DT, Prodhom B, Reiher WE, Roux B, Schlenkrich M, Smith JC, Stote R, Straub J, Watanabe M, Wiorkiewicz-Kuczera J, Yin D and Karplus M (1998) All-atom empirical potential for molecular modeling and dynamics studies of proteins. *J Phys Chem B* **102**(18): 3586-3616.

Maragliano L and Vanden-Eijnden E (2006) A temperature accelerated method for sampling free energy and determining reaction pathways in rare events simulations. *Chem Phys Lett* **426**(1-3): 168-175.

Overington JP, Al-Lazikani B and Hopkins AL (2006) Opinion - How many drug targets are there? *Nat Rev Drug Discov* **5**(12): 993-996.

Rodríguez D, Piñeiro Á and Gutiérrez-de-Terán H (2011) Molecular Dynamics Simulations Reveal Insights into Key Structural Elements of Adenosine Receptors. *Biochemistry* **50**(19): 4194-4208.

Schmidtke P, Luque FJ, Murray JB and Barril X (2011) Shielded hydrogen bonds as structural determinants of binding kinetics: application in drug design. *J Am Chem Soc* **133**(46): 18903-18910.

Shaw DE, Dror RO, Salmon JK, Grossman JP, Mackenzie KM, Bank JA, Young C, Deneroff MM, Batson B, Bowers KJ, Chow E, Eastwood MP, Ierardi DJ, Klepeis JL, Kuskin JS, Larson RH, Lindorff-Larsen K, Maragakis P, Moraes MA, Piana S, Shan Y and Towles B (2009) Millisecond-Scale Molecular Dynamics Simulations on Anton, in *Proceedings of the Conference on High Performance Computing, Networking, Storage and Analysis*, New York.

Smith PK, Krohn RI, Hermanson GT, Mallia AK, Gartner FH, Provenzano MD, Fujimoto EK, Goeke NM, Olson BJ and Klenk DC (1985) Measurement of protein using bicinchoninic acid. *Anal Biochem* **150**(1): 76-85.

Tautermann CS, Kiechle T, Seeliger D, Diehl S, Wex E, Banholzer R, Gantner F, Pieper MP and Casarosa P (2013) Molecular basis for the long duration of action and kinetic selectivity of tiotropium for the muscarinic m3 receptor. *J Med Chem* **56**(21): 8746-8756.

Wang T and Duan Y (2007) Chromophore channeling in the G-protein coupled receptor rhodopsin. *J Am Chem Soc* **129**(22): 6970-6971.

Molecular Pharmacology Fast Forward. Published on February 12, 2016 as DOI: 10.1124/mol.115.102657
This article has not been copyedited and formatted. The final version may differ from this version.

Footnotes

* This work was supported by the Innovational Research Incentive Scheme of the Netherlands Research Organization [Grant 11188]

Current address:

Dong Guo: Jiangsu Key Laboratory of New Drug Research and Clinical Pharmacy, Xuzhou Medical College, 209 Tongshan Road, Xuzhou 221004, Jiangsu, China.

Ron O. Dror: Departments of Computer Science and of Molecular and Cellular Physiology, and Institute for Computational and Mathematical Engineering, Stanford University, Stanford, CA 94305, USA: ROD

Tamara Mocking: Amsterdam Institute for Molecules, Medicines and Systems, VU University Amsterdam, 1081 HV Amsterdam: TM

Molecular Pharmacology Fast Forward. Published on February 12, 2016 as DOI: 10.1124/mol.115.102657
This article has not been copyedited and formatted. The final version may differ from this version.

Figure legends

Fig. 1. Molecular dynamics simulation based on PDB entry 4EIY. A contact was identified when either the oxygen atom in the furan ring (red atom) or the nitrogen atom of the exocyclic amine group (blue atoms) of ZM241385 (inset) was within 4 Å of the backbone nitrogen or carbonyl oxygen of a receptor residue. The ZM241385-A_{2A}R binding pathway passes through multiple distinct consecutive steps, represented by three superimposed snapshots: red (initial pose, 0 ns), green (28 ns) and magenta (32 ns). This figure was generated with ICM Browser v3.8 (Molsoft) from snapshots exported from VMD v1.9.1

Fig. 2. The expression level of the transiently transfected wild-type and mutant adenosine A_{2A} receptors at the surface of human embryonic kidney 293 (HEK293) cells and their interaction with [^{3}H]-ZM241385. (**A**) Expression level of transiently transfected wild-type and mutant adenosine A_{2A} receptors at the surface of HEK293 cells as determined in an ELISA assay. Data are the mean ± s.e.m of at least three independent experiments, each performed in quadruplicate. (**B**) Displacement of [^{3}H]-ZM241385 by increasing concentrations of ZM241385 at the wild-type and mutant adenosine A_{2A} receptors (E169Q and T256A). Data are the mean ± s.e.m of three independent experiments, each performed in duplicate. (**C**) Dissociation of [^{3}H]-ZM241385 from the wild-type and several representative mutant adenosine A_{2A} receptors. Data are the mean ± s.e.m of three independent experiments, each performed in duplicate.

Fig. 3. Amino acid residues having (potential) interactions with ZM241385 during its dissociation process. **(A**) Hydrogen bond network formed by E169, T256, H264 and structural water molecule W2517 in the PDB entry 4EIY. This triad forms a 'lid' probably obstructing ZM241385's dissociation; L267, Y271, I66 and S67 are residues having potential interactions

Molecular Pharmacology Fast Forward. Published on February 12, 2016 as DOI: 10.1124/mol.115.102657
This article has not been copyedited and formatted. The final version may differ from this version.

with ZM241385 during its dissociation. This figure was generated with ICM Browser v3.8 (Molsoft) from PDB entry 4EIY. (**B**) Comparison of ZM241385's pose (magenta) after one representative molecular dynamics simulation (beige, 23 ns) with ZM241385 (orange) bound in the $A_{2A}R$ crystal structure (grey, 0 ns); the pink arrow represents the observation that H264 toggles between different poses during ZM241385 dissociation. This figure was generated with ICM Browser v3.8 (Molsoft) from snapshots exported from VMD v1.9.1(Humphrey et al., 1996).

Molecular Pharmacology Fast Forward. Published on February 12, 2016 as DOI: 10.1124/mol.115.102657
This article has not been copyedited and formatted. The final version may differ from this version.

Tables

Table 1: Molecular dynamics simulation based on PDB entry 4EIY. A contact was identified when either the oxygen atom in ZM241385's furan ring or the nitrogen atom of ZM241385's exocyclic amine group was within 4 Å of the backbone nitrogen or carbonyl oxygen of a receptor residue.

Number	Residue	Location
1	$Q157^{ECL2}$	ECL2
2	$S156^{ECL2}$	ECL2
3	$Y271^{7.36}$	H7
4	$S67^{2.64}$	H2
5	$K153^{ECL2}$	ECL2
6	$G\text{-}1^{N\text{-}term}$	N-term
7	$H264^{7.29}$	H7
8	$A265^{7.30}$	H7
9	$T68^{2.65}$	H2
10	$L267^{7.32}$	H7
11	$E169^{ECL2}$	ECL2
12	$Q148^{ECL2}$	ECL2
13	$G152^{ECL2}$	ECL2
14	$I66^{2.63}$	H2
15	$T256^{6.58}$	H6
16	$P266^{7.31}$	H7

Molecular Pharmacology Fast Forward. Published on February 12, 2016 as DOI: 10.1124/mol.115.102657
This article has not been copyedited and formatted. The final version may differ from this version.

Table 2: Affinity values and dissociation characteristics of ZM241385 at the wild-type (WT) and mutant adenosine A_{2A} receptors.

Mutant	pK_i (M)	Difference from WT (pK_i units)	k_{off} (min^{-1}) [a]	Fold over WT (k_{off})	RT (min) [b]
WT	7.83 ± 0.04	0.00	0.0119 ± 0.0006	1.00	84 ± 2
$I66^{2.63}A$	7.84 ± 0.04	0.01	0.0071 ± 0.0002	0.60	141 ± 2
$S67^{2.64}A$	7.93 ± 0.04	0.10	0.0077 ± 0.0004	0.64	130 ± 4
$T68^{2.65}A$	7.85 ± 0.04	0.02	0.0113 ± 0.0004	0.95	89 ± 2
$Q148^{ECL2}A$	7.78 ± 0.05	–0.05	0.0148 ± 0.0009	1.24	68 ± 2
$K153^{ECL2}A$	7.91 ± 0.05	0.08	0.0094 ± 0.0005	0.79	106 ± 3
$S156^{ECL2}A$	7.98 ± 0.06	0.15	0.0128 ± 0.0007	1.08	78 ± 3
$Q157^{ECL2}A$	8.03 ± 0.06*	0.20	0.0112 ± 0.0006	0.94	89 ± 3
$E169^{ECL2}A$	N/A	N/A	N/A	N/A	N/A
$E169^{ECL2}Q$	7.46 ± 0.04****	–0.37	0.7329 ± 0.0616****	61.6	1.4 ± 0.1
$T256^{6.58}A$	7.43 ± 0.05****	–0.40	0.1994 ± 0.0120****	16.8	5.0 ± 0.2
$H264^{7.29}A$	7.69 ± 0.05	–0.14	0.2235 ± 0.0096****	18.8	4.5 ± 0.1
$L267^{7.32}A$	7.78 ± 0.04	–0.05	0.0051 ± 0.0002	0.43	196 ± 5
$Y271^{7.36}A$	N/A	N/A	N/A	N/A	N/A

Data are represented as mean ± S.E.M. of three separate experiments each preformed in duplicate. Significantly different from wild-type with * $p < 0.05$, **** $p < 0.0001$ (one-way ANOVA with Dunnett's test). [a] Obtained by fitting data into the model of *one-phase exponential decay*. [b] Residence time RT = 1 / k_{off} (k_{off} from one-phase exponential decay); N/A, not available.

Figure 1

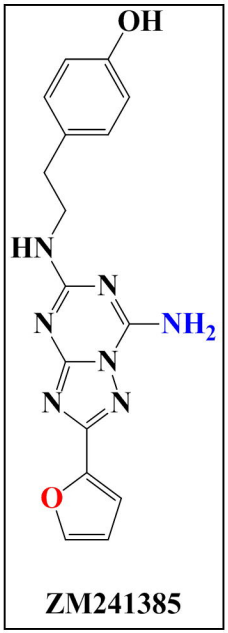

Figure 2

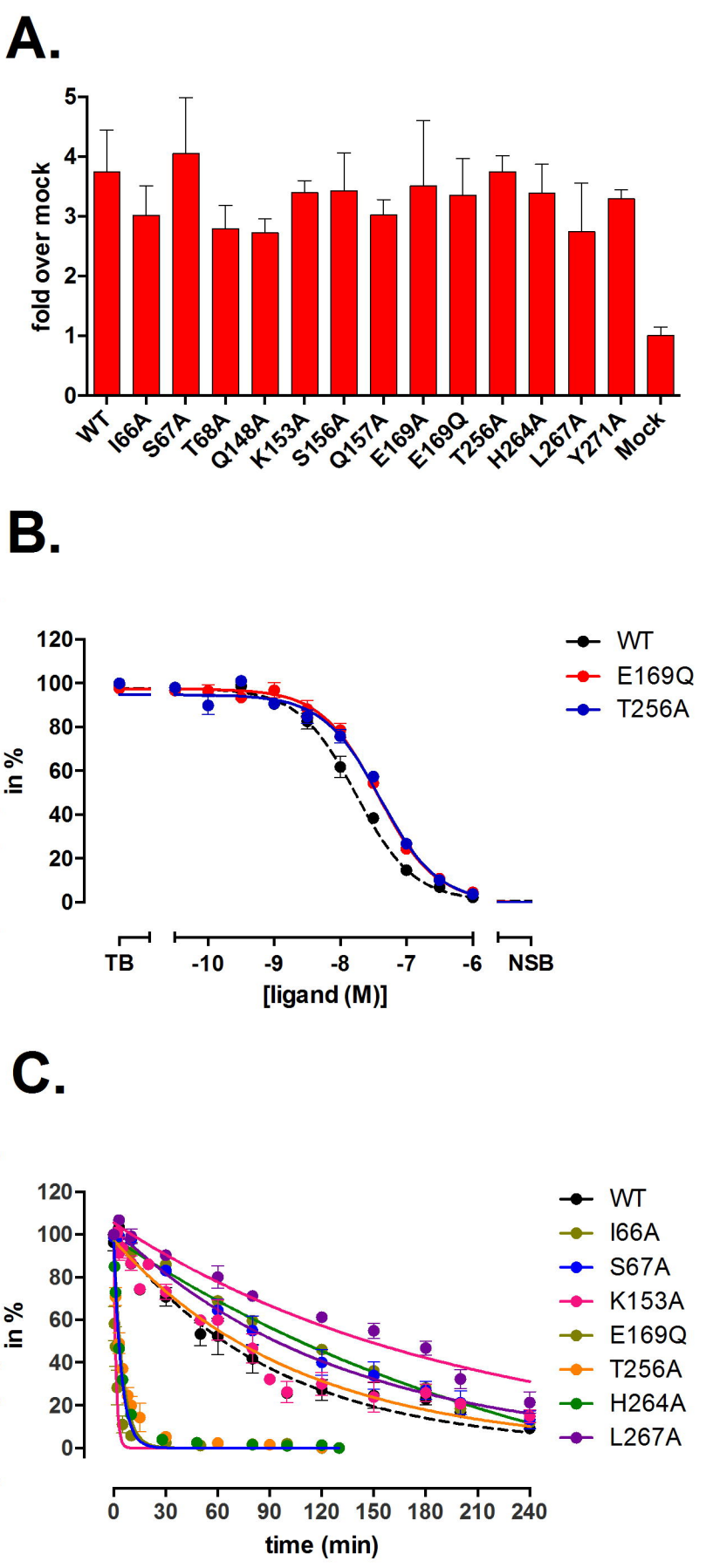
A.
fold over mock
0
1
2
3
4
5
WT
I66A
S67A
T68A
Q148A
K153A
S156A
Q157A
E169A
E169Q
T256A
H264A
L267A
Y271A
Mock
B.
Specific [3H]-ZM241385 binding in %
0
20
40
60
80
100
120
TB
-10
-9
-8
-7
-6
NSB
[ligand (M)]
WT
E169Q
T256A
C.
Specific [3H]-ZM241385 binding in %
0
20
40
60
80
100
120
0
30
60
90
120
150
180
210
240
time (min)
WT
I66A
S67A
K153A
E169Q
T256A
H264A
L267A

Figure 3